Observation of direct and phonon-assisted indirect transitions in $GaAs/Ga_xAl_{1-x}As$ multiquantum wells under hydrostatic pressure

N. Dai and D. Huang
National Key Laboratory for Infrared Physics, Shanghai Institute of Technical Physics, Chinese Academy of Sciences, Shanghai 200083, People's Republic of China
and T. D. Lee Laboratory, Department of Physics, Fudan University, Shanghai 200433, People's Republic of China

X. Q. Liu, Y. M. Mu, W. Lu, and S. C. Shen
National Key Laboratory for Infrared Physics, Shanghai Institute of Technical Physics, Chinese Academy of Sciences, Shanghai 200083, People's Republic of China

(Received 4 June 1997; revised manuscript received 21 August 1997)

Using photomodulated transmission spectroscopy we investigated the interband transitions in $GaAs/Ga_{1-x}Al_xAs$ multiquantum wells as a function of hydrostatic pressure up to 50 kilobar. A number of spectral structures, associated with the Γ, L, and X critical points in GaAs wells and $Ga_{1-x}Al_xAs$ barriers were observed, and calculations were performed to help understanding their origins. The pressure coefficients of the direct transitions in the quantum wells fall between those of GaAs and $Ga_{1-x}Al_xAs$ bulk. The observation of phonon-assisted indirect transitions is made easy by photomodulated transmission technique, and by the band folding effect in the multiple-quantum-well systems. The indirect transitions derived from the L conduction subbands and Γ valence subbands have been observed in wide pressure ranges. [S0163-1829(98)01503-3]

I. INTRODUCTION

$GaAs/Ga_{1-x}Al_xAs$ multiple quantum well's (MQWs) have been intensively studied due to their potential importance for photonic devices. Various optical techniques, such as Raman scattering,[1] photoluminescence (PL),[2] modulation spectroscopy,[3–6] etc., were used to investigate the system under atmospheric pressures. There are also some reports of PL, photoreflectance (PR), and photomodulated transmission spectroscopy (a photomodulated technique in transmission geometry) studies on the system under high pressure.[7–11] Having the advantage of high sensitivity and resolution, modulation spectroscopy has been widely used in studying the interband transitions associated with both the ground and excited states with high accuracy because of the derivative feature of the spectra.[12]

Photoreflectance studies on $GaAs/Ga_{1-x}Al_xAs$ MQW's under hydrostatic pressure was previously reported in Refs. 9 and 10. In their systems, large well widths of 40 and 26 nm were adopted so that a number of transitions, associated with the subbands with quantum indexes up to 8 or 9, were observed. Weak indirect transitions derived from L- and X-band minima were thus overwhelmed by rich direct ones at the Γ critical point that dominated the PR spectra. In those experiments, very few data points related to L and X valleys were resolved.

Photomodulated transmission (PT) spectroscopy was previously performed on $In_xGa_{1-x}As/GaAs$ MQW samples under different hydrostatic pressure.[13] For weak indirect transitions involving a phonon, modulated transmission spectroscopy has better sensitivity than modulated reflectance sensitivity.[11,14,15] Besides, the band-folding effect in superlattices (SL's) and MQW's is also helpful for the enhancement of the weak indirect transitions by making the indirect transition approximately ''direct.'' In this paper, we report an investigation of interband transitions in $GaAs/Ga_{1-x}Al_2As$ MQW's under hydrostatic pressure ranging from 0 to 50 kilobar using PT spectroscopy. A number of spectral structures related to Γ, L, and X valleys are observed.

II. THEORETICAL BACKGROUND

An indirect transition must be phonon or impurity assisted. A phonon or an impurity taking part in the transition supplies a proper momentum to ensure the momentum conservation. As a second-order process, indirect transitions are usually much weaker than direct ones. Based on a second-order perturbation calculation in which the lattice vibration and the radiation field are acting on the electron and hole system, a formula of the indirect transition probability can be given, quantum mechanically, by[16]

$$W(k)=\int_f \frac{1}{\hbar}\,|S_{1-}+S_{1+}+S_{2-}+S_{2+}|^2\,\delta(E_f-E_i)\,dS_f, \tag{1}$$

where

$$S_{1\pm}=\frac{\langle b\mathbf{k}\pm\mathbf{q}|H_v^{\pm}|a\mathbf{k}\pm\mathbf{q}\rangle\langle a\mathbf{k}\pm\mathbf{q}|H_{\mathrm{ep}}^{\pm}|a\mathbf{k}\rangle}{E_g^{\mathbf{k}+\mathbf{q}}-\hbar\omega}, \tag{2}$$

$$S_{2\pm}=\frac{\langle b\mathbf{k}\pm\mathbf{q}|H_{\mathrm{ep}}^{\pm}|b\mathbf{k}\rangle\langle b\mathbf{k}|H_v^{\pm}|a\mathbf{k}\rangle}{E_g^{\mathbf{k}}-\hbar\omega}. \tag{3}$$

Here $H_v^{\pm}$ is the Hamiltonian for electron-photon interaction corresponding to absorbing $(+)$ or emitting $(-)$ a phonon, $H_{\mathrm{ep}}^{\pm}$ represents the electron-phonon interaction for phonon absorption $(+)$ or emission $(-)$. $E_g^{\mathbf{k}}$ $(E_g^{\mathbf{k}+\mathbf{q}})$ is the direct band

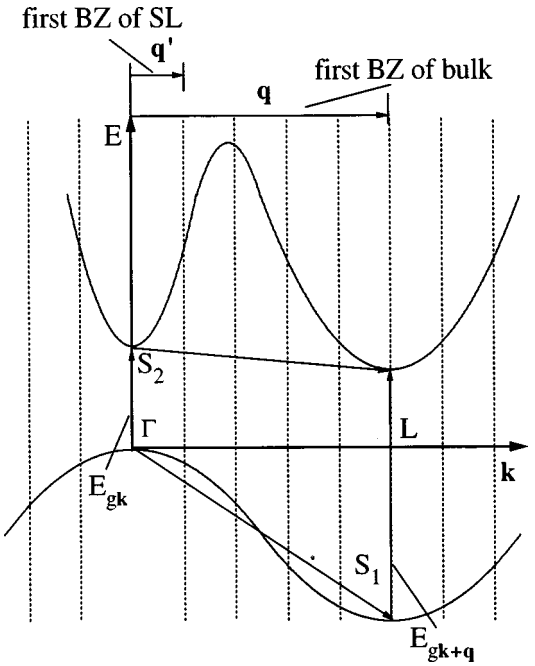

FIG. 1. Indirect transition through virtual processes. In bulk, an optical phonon with large momentum **q** is required, while in a superlattice, the required momentum $\mathbf{q}'$ is made much smaller due to the folding effect. The vertical dashed lines represent the boundaries of the superlattice Brillouin zones (BZ's).

gap at **k** (**k**+**q**). In bulk semiconductors, usually $E_g^{\mathbf{k}}=E_g^{\Gamma}$ (**k**=0) and $E_g^{\mathbf{k}+\mathbf{q}}=E_g^{L}$ or E_g^{X}, i.e., the phonon momentum is at the boundary of the Brillouin zone, as shown in Fig. 1. In GaAs E_g^{Γ} equals 1.42 eV, whereas $E_g^{L}\sim 3$ eV. $E_g^{\mathbf{k}}-\hbar\omega$ is thus much smaller than $E_g^{\mathbf{k}+\mathbf{q}}-\hbar\omega$, so that $S_{1\pm}$ can be ignored. In SL's and MQW's, however, due to the band-folding effect,[17] the momentum **q** of a phonon taking part in a given indirect transition is much smaller than that in the bulk (depending on the period of the SL's and MQW's, as shown in Fig. 1), making the denominators on the right sides of Eqs. (2) and (3) comparable in magnitude. The indirect transitions can thus be enhanced through decreasing the denominator in Eq. (2). Furthermore, the band-folding effect also enhances the matrix elements $\langle a\mathbf{k}\pm\mathbf{q}|H_{\mathrm{ep}}^{\pm}|a\mathbf{k}\rangle$ and $\langle b\mathbf{k}\pm\mathbf{q}|H_{\mathrm{ep}}^{\pm}|b\mathbf{k}\rangle$ in Eqs. (2) and (3). Although $|a\mathbf{k}\rangle(|b\mathbf{k}\rangle)$ is a slow-varying function of **k** and **q**, **q** is a large number in bulk so that the overlap between $|a\mathbf{k}\rangle$ and $|a\mathbf{k}\pm\mathbf{q}\rangle$ ($|b\mathbf{k}\rangle$ and $|b\mathbf{k}\pm\mathbf{q}\rangle$) is very small. In SL's, however, the required $\mathbf{q}'$ is between 0 and one nth of bulk **q** (n is the number of lattices in a SL period) due to the band-folding effect, leading to the enhancement of $\langle a\mathbf{k}\pm\mathbf{q}|H_{\mathrm{ep}}^{\pm}|a\mathbf{k}\rangle$ and $\langle b\mathbf{k}\pm\mathbf{q}|H_{\mathrm{ep}}^{\pm}|b\mathbf{k}\rangle$.

In modulation absorption experiments, one measures $\Delta T/T$, which can be written in terms of absorption coefficient α and extinction coefficient K by[18]

$$\frac{\Delta T}{T}=-\frac{2R}{1-R}\frac{\Delta R}{R}-d\Delta\alpha \tag{4}$$

$$\sim-\frac{2R}{1-R}\frac{\Delta R}{R}-4\pi d\Delta K\frac{1}{\lambda} \tag{5}$$

where T is the transmissivity, R the reflectivity, and d the thickness of the sample. In deriving Eqs. (4) and (5), we have assumed that $\exp(2\alpha d)\gg R^2$, which can be easily satisfied at the energy below and near the indirect transition if the thickness of the specimen is not too thin. In modulated reflectance spectroscopy one measures $\Delta R/R$, which can be described by[18]

$$\frac{\Delta R}{R}=\frac{4(n^2-K^2-1)\Delta n+8nK\Delta K}{[(n+1)^2+K^2][(n-1)^2+K^2]}, \tag{6}$$

assuming normal incidence of light for simplicity. Near the indirect transition energy it satisfies that $n\gg K$, so we have

$$\frac{\Delta R}{R}=\frac{4\Delta n}{n^2} \tag{7}$$

$$\sim\frac{4\Delta K}{n^2}, \tag{8}$$

since $\Delta n\sim\Delta K$. For GaAs, n^2 is typically around 10, $\Delta T/T$ is thus at least one order of magnitude larger than $\Delta R/R$.

Our motivation to carry out this study is based on the above arguments that the use of photomodulated spectroscopy in transmission geometry and the band-folding effect may lead to the great potential for the observation of the weak indirect transitions in GaAs/$Ga_{1-x}Al_xAs$ MQW's.

III. SAMPLE PREPARATION AND EXPERIMENTAL APPARATUS

The samples used in this study were grown by molecular-beam epitaxy on (001) GaAs substrates. A GaAs buffer layer (1 μm in thickness) was deposited on the substrate after thermal deoxidation. The MQW system consisted of 50 periods of a 4-nm GaAs well sandwiched between 30-nm $Ga_{1-x}Al_xAs$ barriers (called $S01$), or a 7-nm well between two 30-nm barriers (called $S02$). The growth temperature for the MQW systems was 550 °C. To carry out the measurement in transmission geometry, the thick GaAs substrate and the buffer had to be removed. A 0.2-μm AlAs spacer was grown between the MQW system and the GaAs buffer, and a 1:4 HF:H_2O solution was used to selectively etch away the AlAs spacer to obtain MQW structures free from the substrates. The free-standing MQW system had a total thickness of about 2000 nm, and was cut into a size of 150 $\times$150 μm^2. The sample was mounted into a high-pressure diamond-anvil cell (DAC) together with a piece of ruby chip for pressure calibration. Hydrostatic pressure was applied by the DAC through a 4:1 methernol-ethanol liquid mixture as pressure transmission medium.

The main part of the setup for PT experiments is shown in Fig. 2. The beam of the 477.2-nm line of an Ar-ion laser was focused on the sample in the DAC with a size of 50 μm in diameter. The probe beam was focused on the sample through lens 2, and penetrated through the sample in the opposite direction of the laser beam. Unlike PR experiments, where reflected light is collected, in PT experiments the transmission light is detected. The probe beam was focused on the input slit of a 0.5-M monochromator and then detected by a photomultiplier tube. Other components of the setup were similar to those in a conventional PR experiment.

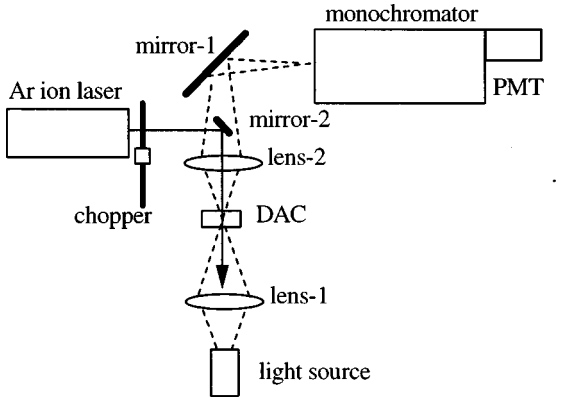

FIG. 2. Experimental setup for photomodulated transmission spectroscopy.

IV. RESULTS AND DISCUSSION

PT spectra measured on $S01$ and $S02$ at several pressure values are presented in Fig. 3. The spectra show distinct structures associated with the subband transitions in the GaAs quantum wells and band-edge transitions in the $Ga_{1-x}Al_xAs$ barriers. The transition from the mth subband in the heavy-hole (light-hole) valence band (VB) to the nth-electron subband in the conduction band (CB) is labeled by $nmH^i(L^i)$, where i equals Γ, L, or X, indicating the region in the Brillouin zone from which the transitions derive. On both samples, only allowed transitions ($n=m$) are observed. E_g^Γ, E_g^L, and E_g^X denote the direct band gap of the $Ga_{1-x}Al_xAs$ barriers at Γ, the indirect band gap between L CB minima and the Γ VB maximum, and the indirect band gap between X CB minima and the Γ VB maximum, respectively. In order to make it easy to resolve relatively weak indirect transitions on PT spectra, the 4-nm (7-nm) well thickness was chosen for $S01$ ($S02$), so that QW's in the CB could accommodate only one (two) confined state. The observation of the indirect transitions relies on pressure. Increasing the hydrostatic pressure leads to the appearance of more spectral structures, as shown in Fig. 3.

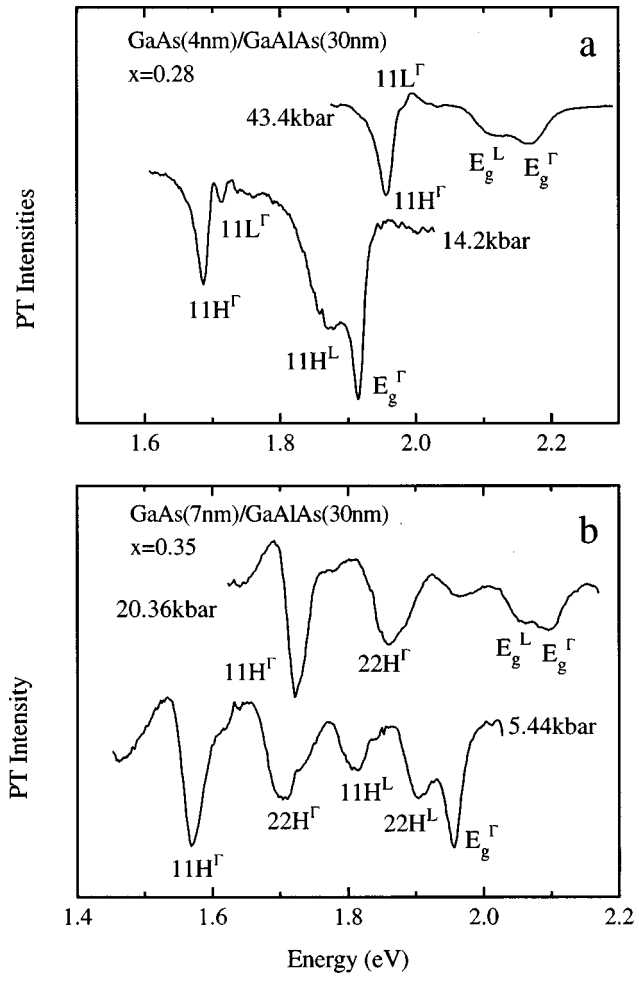

FIG. 3. Photomodulated transmission spectra measured at 14.2 and 43.4 kbar for $S01$ (a), and at 5.4 and 20.4 kbar for $S02$ (b).

Some material and structural parameters of $S01$ and $S02$ can be estimated in terms of the PT results. According to Casey and Panish,[19] the compositional dependence of the energy gaps (E_g's) in $Ga_{1-x}Al_xAs$ can be expressed at 300 K by

$$E_g^\Gamma = 1.424 + 1.247x \quad (0 \leqslant x \leqslant 0.45), \tag{9}$$

$$= 1.424 + 1.247x + 1.147(x-0.45)^2 \quad (0.45 < x \leqslant 1.0) \tag{10}$$

for the Γ direct band gap ($\Gamma_6^c - \Gamma_8^v$), as well as

$$E_g^L = 1.708 + 0.642x, \tag{11}$$

$$E_g^x = 1.900 + 0.125x + 0.143x^2 \tag{12}$$

for the L ($L_6^c - \Gamma_8^v$) and X ($X_6^c - \Gamma_8^v$) indirect gaps, respectively. In terms of Eq. (9), the band-gap energy of the $Ga_{1-x}Al_xAs$ barriers determined from the zero pressure PT spectra, x, and then indirect gaps E_g^L and E_g^X, were calculated using Eqs. (11) and (12). Thus the potential profiles regarding the Γ valence band and the Γ, L, and X conduction bands could be obtained (see Fig. 4).

It has been recognized that within the quantum wells the transition is excitonic, which differs energetically from the corresponding band-edge transition by an exciton binding energy. However, the situation is made complicated by the fact that in quantum wells the binding energy of an exciton depends both on the well width and barrier height. Confined in an ideal two-dimensional system (an infinitely high barrier and infinitely narrow well), an exciton has a binding energy of 4 Ry instead of 1 Ry in bulk. Thus the exciton binding energy values between 1 and 4 Ry in a practical quantum well. Quite a number of theoretical and experimental efforts have been devoted to study the well-width and barrier-height dependences of the exciton binding energy.[20–22] It is estimated that the confinement-induced increase in the exciton binding energy is around 4–5 meV in our GaAs/$Ga_{1-x}Al_xAs$ MQW systems. We use a binding energy of 10 meV for direct excitons at the Γ point (the binding energy in the GaAs bulk is about 5 meV), which is a reasonable value as shown by a number of calculations and experiments.[20–22]

In terms of the potential profiles depicted in Fig. 4, the peak energies of the transitions inside the quantum wells

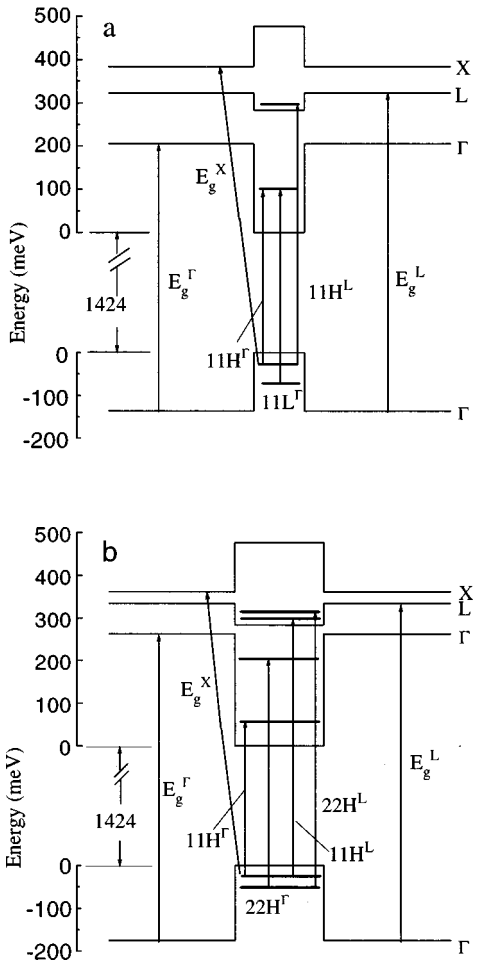

FIG. 4. Calculated band alignment of $S01$ and $S02$ using the parameters listed in Table I.

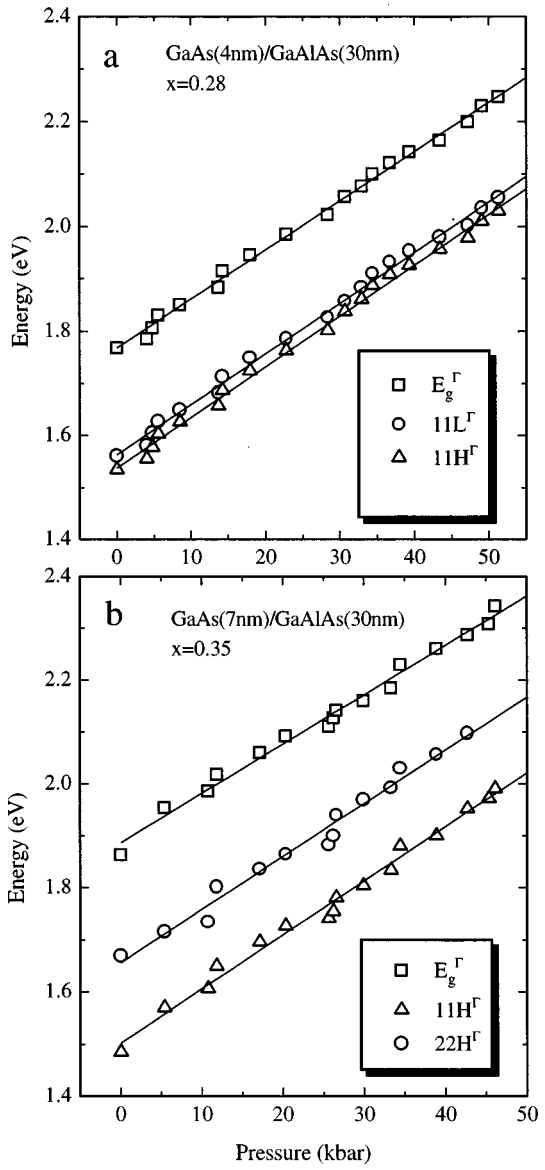

FIG. 5. The energies of direct transitions in the Γ vicinity as a function of hydrostatic pressure for $S01$ (a) and $S02$ (b). The straight lines are the least-square fits to the experimental data.

were calculated in the transfer-matrix-element (TME) scheme,[23] using the well thickness as a fitting parameter. The band-edge parameters were used in the calculation, except that a 10-meV exciton binding energy was included to count in the exciton effect. For the indirect transitions the exciton binding energies were ignored, since they were much smaller than those of the direct ones. The material parameters used in the calculation are tabulated in Table I. The well widths for both samples are in good agreement with those estimated from the growth parameters. Calculated energies for various transitions in $S01$ and $S02$ are marked by arrows in Fig. 4.

1. Direct transitions at Γ band edges

The energies vs hydrostatic pressures for several direct transitions observed by PT measurements are summarized in Figs. 5(a) and 5(b). The solid lines in the figures are the least-square fits to the experimental data, assuming a linear energy-pressure relation of

$$E^i(P)=E^i(0)+\frac{\partial E^i}{\partial P}P. \tag{13}$$

Here $E^i(0)$ is the transition energy at zero pressure, $\partial E^i/\partial P$ is the pressure coefficient, and i denotes various transitions such as $11H^\Gamma$, $11L^\Gamma$, etc. The pressure coefficients and zero-pressure transition energies, obtained from the least-square fit to the experimental data in Figs. 5(a) and 5(b), are listed in Table II.

In GaAs/$Ga_{1-x}Al_xAs$ MQW systems, potential wells are formed in GaAs layers, and the electronic states are characterized by quantized subbands whose energy positions rely on the GaAs well width and the $Ga_{1-x}Al_xAs$ barrier height. The observed $11H^\Gamma$ is derived from the first electron state and the first heavy-hole state at the Γ point, both states being

TABLE I. The sample parameters used in the TME calculation. The well and barrier widths are in nm, and the band gaps and band offsets in eV. The CB (VB) offset ratio $\Delta E_c/\Delta E_g(\Delta E_c/\Delta E_g)$ is taken as 60% (40%).

	L_W	L_B	x	ΔE_c	ΔE_v
$S01$	3.9	30	0.275	0.206	0.137
$S02$	6.5	30	0.350	0.262	0.175

TABLE II. The pressure coefficients and zero-pressure transition energies obtained by least-square fits to the pressure dependence of various transitions measured on $S01$ and $S02$. (The transition energies are in eV, and the pressure coefficients in meV/kbar).

	$S01$ E_0^i	$S01$ $\partial E^i/\partial P$	$S02$ E_0^i	$S02$ $\partial E^i/\partial P$	GaAs bulk $\partial E^i/\partial P$
$11H^{\Gamma}$	1.537	9.73	1.501	10.40	
$11L^{\Gamma}$	1.562	9.70			
$22H^{\Gamma}$			1.656	10.22	
$11H^{L}$	1.821	3.48	1.786	3.17	
$22H^{L}$			1.875	4.67	
$E_g^L(Ga_{1+x}Al_xAs)$	1.981	3.00	2.007	2.58	
$E_g^{\Gamma}(Ga_{1-x}Al_xAs)$	1.768	9.39	1.887	9.45	
E_g^{Γ}(GaAs)					10.73[a](10.8[b])

[a]Reference 25.
[b]Reference 26.

confined in the GaAs well layers. The pressure coefficient of the $11H^{\Gamma}$ transition, as listed in Table II, falls between those of the $Ga_{1-x}Al_xAs$ and GaAs bulk, which can be interpreted as due to a wave function penetrating into the $Ga_{1-x}Al_xAs$ barriers that have a slightly smaller pressure coefficient than GaAs. In the table, the pressure coefficients of E_g^{Γ} are obtained from the measured pressure dependence of the fundamental band gaps of the $Ga_{1-x}Al_xAs$ barrier layers in $S01$ and $S02$. It has been recognized that the pressure coefficient of $Ga_{1-x}Al_xAs$ depends on x in a quite complicated way.[24] The pressure coefficients for GaAs in Table II are cited from Refs. 25 and 26, respectively. Note the slight divergence of the pressure coefficients between publications.[25–28] Since the heavy-hole excitons are strongly localized in the well regions (GaAs layers), the pressure coefficient of $11H^{\Gamma}$ is expected to be close to that of the band-edge transition in the GaAs bulk. The slightly different pressure coefficients of $11H^{\Gamma}$ for $S01$ and $S02$ are due to their different well widths as well as different Al concentration in the barrier layers. $S01$ has a narrower well width and a lower Al concentration in the barriers. The former tends to decrease the pressure coefficient, while the latter tends to increase it. The larger pressure coefficient of $11H^{\Gamma}$ in $S02$ indicates that, in our case, the former is more significant than the latter.

Compared to heavy holes, light holes are less localized, i.e., relatively more wave function penetrates into the $Ga_{1-x}Al_xAs$ barriers, implying that light holes might have a smaller pressure coefficient. However, the pressure coefficients of the light- and heavy-hole excitons do not appear very different since it happens that in GaAs/$Ga_{1-x}Al_xAs$, QWs with $x\sim0.3$ the CB band offset (ΔE_c), takes 90% of the pressure-induced variation of energy-gap difference between GaAs and $Ga_{1-x}Al_xAs$.[29] Another effect, although it is small, is more significant for light holes than for heavy holes. With the increase of pressure the well width tends to decrease, which pushes the light-hole states down, leading to the increase of its pressure coefficient. All this results in approximately the same pressure coefficients for the heavy- and light-hole transitions, as clearly indicated in Fig. 5. The $11L^{\Gamma}$ transition is rather difficult to resolve on $S02$, since the weak peak is overwhelmed by other stronger peaks in its vicinity.

As expected, $22H^{\Gamma}$ has nearly the same pressure coefficient as that of $11H^{\Gamma}$, since the localization of the $n=1$ and the $n=2$ heavy holes are essentially the same for QW's which can accommodate three ($S01$) or four ($S02$) confined heavy-hole states according to our calculations. Note that the small difference between pressure coefficients of $11H^{\Gamma}$ and $22H^{\Gamma}$ is within the error bar in experimentally determining the peak position of $22H^{\Gamma}$. The weak peak intensity as well as the crossover with other stronger peaks makes it difficult to locate its energy positions accurately.

It should be noted that the sublinearity of the pressure dependence of the transition energies does exist in GaAs/$Ga_{1-x}Al_xAs$ QW systems,[10] due to a variety of origins, such as pressure-induced changes in exciton binding energy, effective mass, etc. The sublinearity, however, appears to be significant only at high pressure for transitions derived from high quantum index states. This effect is extremely small for our samples in the studied pressure range.[30,9,10]

2. Phonon-assisted indirect transitions associated with L and X conduction minima

It is rather difficult to resolve the weak L-related indirect transitions on reflectance or modulated reflectance spectra.[9,10] Using the PT technique, several phonon-assisted indirect transitions are clearly observed, as shown in Fig. 3. Summarized in Figs. 6(a) and 6(b) are the transition energies versus hydrostatic pressures obtained from PT measurements (filled triangles, circles, and squares). They are identified as the transitions between the CB minima at the L point and the VB maximum at the Γ point, according to their typical values of L-valley pressure coefficient (see Table II).[9,31] The least-square fits to the experimental data yield pressure coefficients around 3.0–3.4 meV/kbar (see Table II), consistent with the reported values. The indirect transitions gain their intensities as merged from the $11H^{\Gamma}$ peak and, with the further increase of pressure, lose their intensities as approached by other stronger peaks ($11H^{\Gamma}$ or $22H^{\Gamma}$). They become difficult to resolve when the crossover between Γ CB and L CB band edges occurs.

$11H^{L}$ (filled triangles) is identified as the indirect transition between the $n=1$ heavy hole at Γ and $n=1$ electron states at L in the quantum wells. In $S02$, $11H^{L}$ is well resolved even at atmospheric pressure (0 bar), whereas in $S01$ a pressure over 10 kbar is required to reveal the peak. The different behavior of $S01$ and $S02$ can be explained according to the potential profiles of the Γ, L, and X band edges depicted in Fig. 4. The confinement energies for the electrons and holes in quantum wells were calculated by the TME scheme using the corresponding effective masses at Γ, L, and X valleys.[32] It is obvious from Fig. 4 that, in $S02$, due to its relatively large well thickness and high Al concentration in the barrier layers, the $11H^{L}$ peak is roughly 140 meV below E_g^{Γ}, while in $S01$ the corresponding value is 15 meV so that a much higher pressure is required to move $11H^{L}$ far away from E_g^{Γ}.

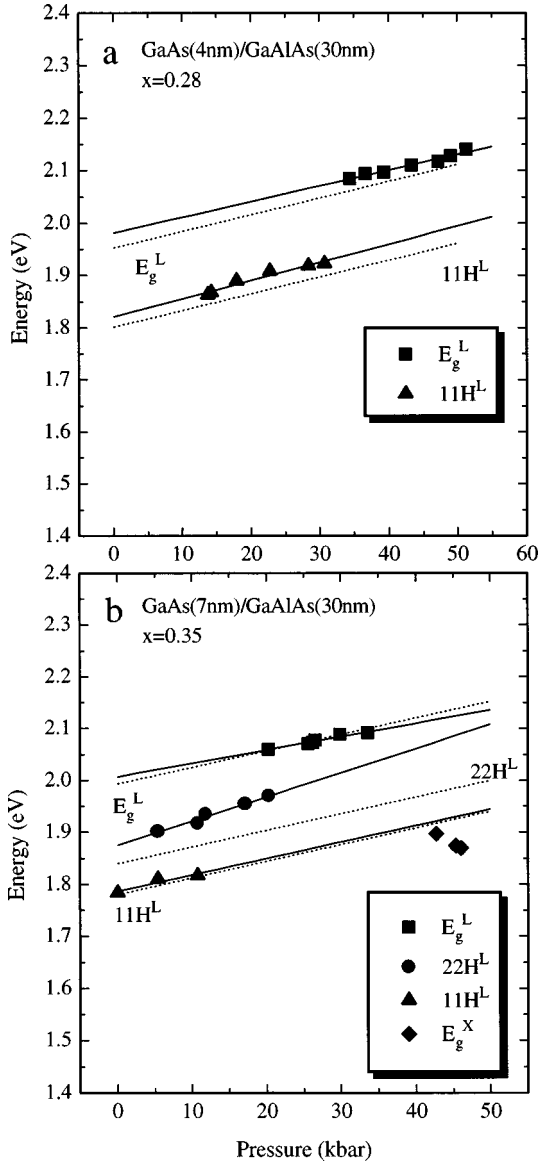

FIG. 6. The energies of indirect transitions derived from L and X conduction minima as functions of hydrostatic pressure measured on $S01$ (a) and $S02$ (b).

In Fig. 6, the dashed line is the calculated transition energy as a function of hydrostatic pressure using a pressure coefficient of 3.20 meV/kbar, and the transition energies at conventional pressure (0 bar) calculated in terms of L-band potential profiles in Fig. 4. An optical-phonon energy of 40 meV is also included in the calculation. Without taking into account the phonon energy, the calculated L indirect transition energies are, quite consistently, 40–60 meV below the experimental ones. Such a discrepancy exceeds the error bar due to the uncertainty in material parameters and the approximation made in the calculations. We thus believe that the second-order perturbation is dominated by phonon emission, so that a phonon energy of 40 meV should be added. For phonon absorption, 40 meV has to be deducted from the calculated transition energies, and the discrepancy is then as large as 100 meV. The inclusion of phonon energy results in a good agreement between calculations and experiments (see Fig. 6). Other factors may contribute to the rest of the 10–20-meV discrepancy. The parameters at the Brillouin zone, other than the Γ valley, including the band gaps (as a function of Al concentration), band alignments (band offsets), etc., are currently known with poor accuracy. E_g's dependence on x, quoted in Refs. 19 and 32, for instance, shows a disagreement of about 15 meV at $x=0.3$. The rest of the error may be due to the uncertainties in determining the well layer thickness and Al concentrations in the barrier layers. Better agreement between the calculations and experiments was expected with the use of more accurate parameters.

In $S02$, another L-related transition shows up in the pressure range between 5 and 20 kbar. This transition is called $22H^L$. While $11H^L$ and E_g^L have roughly the same pressure coefficients, the peak energy of $22H^L$ increases significantly faster than that of $11H^L$ with pressure, which is most likely due to the band mixing with Γ band. The integral peak intensities of $11H^L$ and $22H^L$, though varying with the pressure, may reach to roughly one-third of that of $11H^\Gamma$, as shown in Fig. 3. It should be pointed out that protuberance of the indirect transitions is not only due to the measurement in transmission geometry and band-folding effect, but also the relatively larger joint density of states between the L CB and Γ VB than that between the Γ CB and Γ VB since the L-CB valleys have larger effective mass than the Γ-CB minimum.

A peak merged from $11H^\Gamma$ as the pressure was raised above 45 kbar on $S02$. This transition has the obvious origin of X band ($X_6^c-\Gamma_8^v$) judged by its negative pressure coefficient. This transition has been observed previously on photoreflectance spectra under high pressure.[7,9] We did not observe E_g^X on $S01$ at pressures up to 50 kbar. Based on Fig. 4 for the band alignments of the Γ, L, and X band edges, we expect that an even higher pressure be required to make E_g^X of $S01$ observable.

V. CONCLUSION

In conclusion, using photomodulated transmission spectroscopy, we investigated the transitions in GaAs/$Ga_{1-x}Al_xAs$ multiple quantum wells as a function of hydrostatic pressure up to 50 kilobar. A number of spectral structures associated with both direct and indirect transitions are observed. The pressure coefficients of the direct transitions derived from the confined subbands in GaAs quantum wells are found to fall between those of the GaAs and $Ga_{1-x}Al_xAs$ bulk. The phonon-assisted indirect transitions $11H^L$, $22H^L$, and E_g^L are clearly observed in wide pressure ranges due to the band-folding effect in the multiple-quantum-well systems and with the use of photomodulation technique in transmitting geometry.

ACKNOWLEDGMENT

This work was supported by the Research Foundation of National Key Laboratory for Infrared Physics.

[1] J. E. Zucker, A. Pinczuk, D. S. Chemla, A. Gossard, and W. Wiegmann, Phys. Rev. Lett. **51**, 1293 (1983).
[2] R. C. Miller, D. A. Kleinman, W. A. Nordland, Jr., and A. C. Gossard, Phys. Rev. B **22**, 863 (1980).
[3] H. Shen, S. H. Pan, Z. Hang, J. Leng, F. H. Pollak, J. M. Woodall, and R. N. Sacks, Appl. Phys. Lett. **53**, 1080 (1988).
[4] F. H. Pollak, Proc. Soc. Photo-Opt. Instrum. Eng. **1361**, 109 (1991).
[5] M. Erman, J. B. Theeten, P. Frijlink, S. Gaillard, Fan Jia Hia, and C. Alibert, J. Appl. Phys. **56**, 3241 (1984).
[6] Y. R. Lee, A. K. Ramdas, A. L. Moretti, F. A. Chambers, G. P. Devane, and L. R. Ram-Mohan, Phys. Rev. B **41**, 8380 (1990).
[7] U. Venkateswaren, M. Chandrasekhar, H. R. Chandrasekhar, B. A. Vojak, F. A. Chambers, and J. M. Meese, Phys. Rev. B **33**, 8416 (1986).
[8] U. Venkateswaren, M. Chandrasekhar, H. R. Chandrasekhar, T. Wolfram, R. Fischer, W. T. Masselink, and H. Morkoc, Phys. Rev. B **31**, 4106 (1985).
[9] A. Kangarlu, H. R. Chandrasekhar, and M. Chandrasekhar, Superlatt. Microstruct. **2**, 569 (1986).
[10] M. Chandrasekhar, H. R. Chandrasekhar, A. Kangarlu, and U. Venkateswaran, Superlatt. Microstruct. **4**, 107 (1988).
[11] N. Dai, D. M. Huang, X. Q. Liu, Y. M. Mu, W. Lu, and S. C. Shen, J. Appl. Phys. **82**, 6359 (1997).
[12] D. E. Aspnes, Surf. Sci. **37**, 418 (1973).
[13] W. Shan, X. M. Fang, D. Li, S. Jiang, S. C. Shen, H. Q. Hou, W. Feng, and J. M. Zhou, Phys. Rev. B **43**, 14 615 (1991).
[14] F. Evangelisti, A. Frova, and Margherita Zanini, Solid State Commun. **9**, 1467 (1971).
[15] T. Nishino, M. Takeda, and Y. Hamakawa, J. Phys. Soc. Jpn. **37**, 1016 (1974).
[16] B. K. Ridlay, *Quantum Processes in Semiconduclors* (Clarendon, Oxford, 1982), p. 209.
[17] Jian-Bai Xia, Phys. Rev. B **38**, 8358 (1988).
[18] B. Batz, in *Semiconductors and Semimetals Vol. 9*, edited by R. K. Willardson and A. C. Beer (Academic, New York, 1972), p. 316.
[19] H. C. Casey, Jr. and M. B. Panish, *Heterostructure Lasers* (Academic, New York, 1978), Parts A and B.
[20] J. C. Maan, G. Belle, A. Fasolino, M. Altarelli, and K. Ploog, Phys. Rev. B **30**, 2253 (1984).
[21] H. Mathieu, P. Lefebvre, and P. Christol, Phys. Rev. B **46**, 4092 (1992).
[22] Z. S. Piao, M. Nakayama, and H. Nishimura, Phys. Rev. B **54**, 10 312 (1996).
[23] W. W. Lui and M. Fukuma, J. Appl. Phys. **60**, 1555 (1986).
[24] N. Lifshitz, A. Jayaraman, R. A. Logan, and R. G. Maines, Phys. Rev. B **20**, 2398 (1979).
[25] D. J. Wolford and J. A. Bradley, Solid State Commun. **53**, 1069 (1985).
[26] A. R. Goñi, K. Strössner, K. Syassen, and M. Cardona, Phys. Rev. B **36**, 1581 (1987).
[27] R. B. Capaz, G. C. de Araujo, B. Koiller, and J. P. von der Weid, J. Appl. Phys. **74**, 5531 (1993).
[28] M. Hanfland, K. Syassen, and N. E. Christensen, J. Phys. Colloq. **8**, C-57 (1984).
[29] Z. X. Liu, G. H. Li, H. X. Han, and Z. P. Wang, Chin. J. Semicond. **15**, 163 (1994).
[30] D. L. Camphausen, G. A. N. Connell, and W. Paul, Phys. Rev. Lett. **26**, 184 (1971).
[31] Effective mass at G, L, and X points are calculated using $0.067+0.083x$, $0.56+0.1x$, and $0.85-0.14x$, respectively [S. Adachi, J. Appl. Phys. **58**, R1 (1985].
[32] H. J. Lee, L. Y. Juravel, and J. C. Woolley, Phys. Rev. B **21**, 659 (1980).